Mater. Res. Soc. Symp. Proc. Vol. 1165 © 2009 Materials Research Society 1165-M01-07

Characterizing the effects of silver alloying in chalcopyrite CIGS solar cells with junction capacitance methods

Peter T. Erslev[1], Gregory M. Hanket[2], William N. Shafarman[2], and J. David Cohen[1]
[1]University of Oregon Physics Department, Eugene, Oregon 97405
[2]Institute of Energy Conversion, University of Delaware, Newark, Delaware, 19716

ABSTRACT

A variety of junction capacitance-based characterization methods were used to investigate alloys of Ag into $Cu(In_{1-x}Ga_x)Se_2$ photovoltaic solar cells over a broad range of compositions. These alloys show encouraging trends of increasing V_{OC} with increasing Ag content, opening the possibility of wide-gap cells for use in tandem device applications. Drive level capacitance profiling (DLCP) has shown very low free carrier concentrations for all Ag-alloyed devices, in some cases less than 10^{14} cm^{-3}, which is roughly an order of magnitude lower than that of CIGS devices. Transient photocapacitance spectroscopy has revealed very steep Urbach edges, with energies between 10 meV and 20 meV, in the Ag-alloyed samples. This is in general lower than the Urbach edges measured for standard CIGS samples and suggests a significantly lower degree of structural disorder.

INTRODUCTION

Thin film solar cells based on the alloys of $CuInSe_2$ (CIS) hold substantial promise for an economical source of photovoltaic energy. Because the band gap of CIS (~ 1 eV) does not optimally match the solar spectrum, it is normally alloyed with Ga (CIGS) to produce higher band gaps (up to 1.7 eV for $CuGaSe_2$). Unfortunately, the predicted increase in efficiency for band gaps above roughly 1.2 eV (~ 30% Ga) has not yet been realized, primarily due to a deficit in the open circuit voltage [1]. We have examined several sets of samples in which Ag has been alloyed into CIGS devices as $(Ag_xCu_{1-x})(In_{1-y}Ga_y)Se_2$ (ACIGS) in hopes that such alloys will produce increases in the band gaps beyond 1.2 eV accompanied by correspondingly higher values of V_{OC}. The endpoint $AgInSe_2$ and $AgGaSe_2$ compounds have band gaps 0.1 eV to 0.2 eV higher than the corresponding Cu compounds, so an increase in the band gap of the alloys might be expected. In addition, because the melting point of the Ag compounds are typically 200 °C lower than that of the Cu compounds, one might expect reduced structural disorder for the Ag alloys and thus better electronic properties [2].

CIGS alloys with Ag have thus far received relatively little attention, partially because it had been believed that single phase chalcopyrite compounds could only be produced over a limited range of compositions [3, 4]. This is in spite of the work by Nakada et. al., who produced a 9.3% efficient single phase chalcopyrite $AgInGaSe_2$ device with a 949 mV V_{OC} [5]. However, by employing our co-evaporation deposition process we have been able to deposit uniform single-phase ACIGS absorbers over a broad range of Ag and Ga concentrations. These films were incorporated into working solar cells, with Mo back contacts, and buffer and window layers of CdS, ZnO and ITO. We then employed several junction capacitance methods to characterize their electronic properties. Here we report results on three series of such completed ACIGS devices: One in which the Ag concentration (x) was held constant at 16% and the Ga fraction (y) was varied from 29% to 80%, and two others which employed constant Ga concentrations (50% and 80%) with varying Ag concentrations from 25% to 75%. The device efficiencies were similar to the corresponding alloys without Ag, with a highest efficiency

Table I: ACIGS device performance parameters, plus the free carrier densities and deep acceptor densities determined by DLCP, as well as the Urbach energies obtained from TPC.

Sample	Ag/(Ag+Cu)	Ga/(In+Ga)	V_{OC} (V)	J_{SC} (mA cm^{-2})	*FF* (%)	Eff (%)	p (10^{14} cm^{-3})	N_A (10^{14} cm^{-3})	E_U (meV)
34225	0.16	0.29	0.63	32.8	77.3	16.0	4.0	>8.0	15
34227	0.16	0.45	0.70	30.0	76.4	16.1	1.0	>3.0	14
34228	0.15	0.56	0.73	25.6	68.9	12.8	1.2	>9.0	17
34229	0.16	0.80	0.76	17.7	65.8	8.8	1.8	>9.0	13
34235	0.28	0.30	0.63	30.7	76.1	14.7	1.0	~ 1.0	10
34234	0.28	0.47	0.58	25.8	58.5	8.8	1.0	2.0	13
34244	0.46	0.50	0.75	24.4	72	13.1	0.6	1.2	11
34254	0.76	0.53	0.77	22.4	69	11.8	0.7	2.3	12
34232	0.27	0.81	0.63	18.7	61.5	7.3	1.1	1.9	20
34276	0.50	0.83	0.79	15.9	53	6.5	1.0	3.8	12
34259	0.76	0.81	0.84	16.3	66	9.1	1.0	5.0	15

achieved to date of 16.1 % (V_{OC} = 0.70 V) for a sample device with Ag and Ga fractions of 0.16 and 0.45, respectively. The devices with varying Ag content showed an encouraging trend of higher open circuit voltages with increasing Ag fraction.

SAMPLES

ACIGS films were deposited by elemental co-evaporation using a uniform single-stage growth process in which the incident elemental fluxes were invariant with time. The substrate temperature was 550°C and the films were 2 μm thick. Film compositions were measured by energy dispersive x-ray spectroscopy with 20 kV accelerating voltage in the scanning electron microscope and the composition ratios [Ag]/[Ag+Cu] and [Ga]/[In+Ga] are listed in Table 1. All films were group I deficient with [Ag+Cu]/[In+Ga] = 0.8 – 0.9. Films were further characterized by x-ray diffraction which indicated that all films were single phase. The ACIGS was deposited on Mo-coated soda lime glass substrates. Devices with area 0.47 cm^2 were completed with chemical bath deposited CdS (thickness ≈ 50 nm), sputtered undoped ZnO (50 nm) and ITO (150 nm) and an evaporated Ni/Al grid. Current-voltage measurements listed in Table I were measured under AM1.5 illumination.

CHARACTERIZATION METHODS

Several junction capacitance based techniques were used to investigate these samples. Admittance spectroscopy examines the complex electrical response of the sample to an AC perturbing voltage over a range of frequencies and temperatures. The temperature and frequency of the measurement determine an emission energy $E_e = k_B T \ln(\nu/2\pi f)$ where T is the temperature, ν is the thermal emission prefactor, and f is the measurement frequency.

Drive-level capacitance profiling (DLCP) determines the density of charge that can respond to the applied oscillating voltage by examining the dependence of the capacitance to the amplitude of the AC signal as $C = C_0 + C_1(\delta V) + C_2(\delta V)^2 + \ldots$ The drive level density, N_{DL}, is obtained from the coefficients C_0 and C_1 and is equal to the free carrier density plus an integral over the density of deep defect states to an energy E_e above E_V, and near the spatial position $\langle x \rangle = \varepsilon A/C_0$ from the barrier junction [6]. By varying the frequency and temperature of the measurement, we can thus determine the free carrier density and the deep defect density at

specific locations in the sample. Spatial profiles are then obtained by varying the DC reverse bias. The free carrier density (p) is thus estimated from spatially averaging the lowest temperature, highest frequency DLCP values, and these values are listed in Table I. Standard C-V capacitance profiling methods has been used at a very low-frequency limit to estimate the total concentration of free carriers plus deep acceptors ($p + N_A$). In the lowest Ag-fraction samples, a limiting value was not reached by the C-V profiles, and thus we have given a lower limit for the deep defect density in Table I.

Transient photocapacitance (TPC) spectroscopy provides a sub-band gap optical absorption-like spectrum. A sample is held in steady state under reverse bias, but periodically pulsed to zero bias or slightly forward to "reset" the occupation of defects in the sample. In the case of CIGS this allows the capture of majority carriers (holes) into previously empty traps in the depletion region. After the pulse is removed, we observe the capacitance transient as the carriers are thermally emitted from the occupied traps. A TPC signal is obtained by comparing the transient while the sample is illuminated with monochromatic light to the transient while the sample recovers in the dark. A TPC spectrum is obtained by varying the wavelength of the monochromatic light, and this spectrum is closely related to an integral over the density of states in the band gap, as has been described in detail elsewhere [7]. Such TPC spectra typically exhibit several important features: (1) The exponential distribution of states near the edge of the band gap (characterized by the Urbach energy) depends on the degree of structural and compositional disorder in the sample. (2) The spectra also can disclose the presence of defect states deeper in the band-gap, which are typically well fit by Gaussian distributions.

EXPERIMENTAL RESULTS

The admittance spectra of nearly all of the ACIGS samples in their fully annealed state did not exhibit the usual capacitive step indicative of a deep majority carrier trap, as seen in Figure 1(a). However, once the samples had undergone light-soaking with AM 1.5 white light, there was not only a significant increase in the free carrier density but also an activated step that appeared in the admittance spectra (Figure 1(b)). This capacitance step had activation energies, as determined by an Arrenhius plot, of between 150 meV and 250 meV, very similar to the activation energies obtained for CIGS without Ag. Following light-soaking, this feature started annealing away when the temperature exceeded 250 K, again much like the metastable behavior in CIGS without Ag.

Figure 2 shows the DLCP results from the sample with 28% Ag and 30% Ga. This

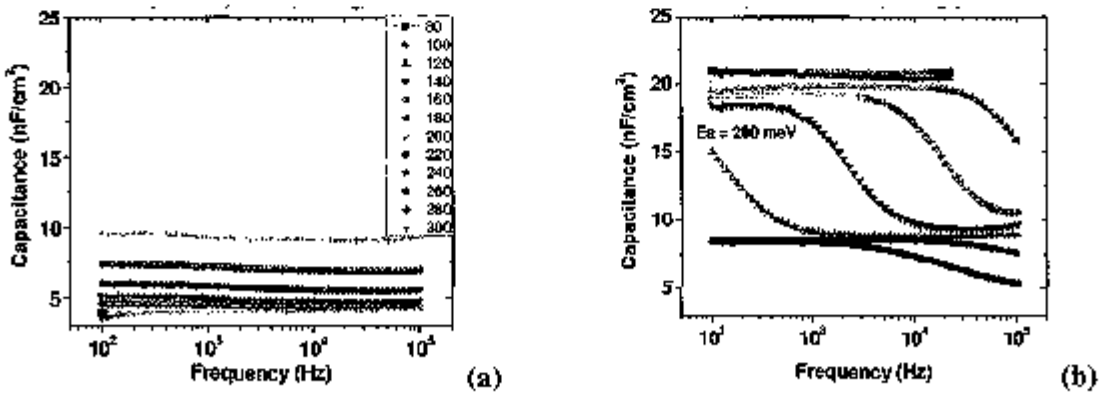

Figure 1: (a) Typical admittance spectra from ACIGS samples showing no defect features in the fully annealed state and (b) an activated step after the sample is light soaked for two hours.

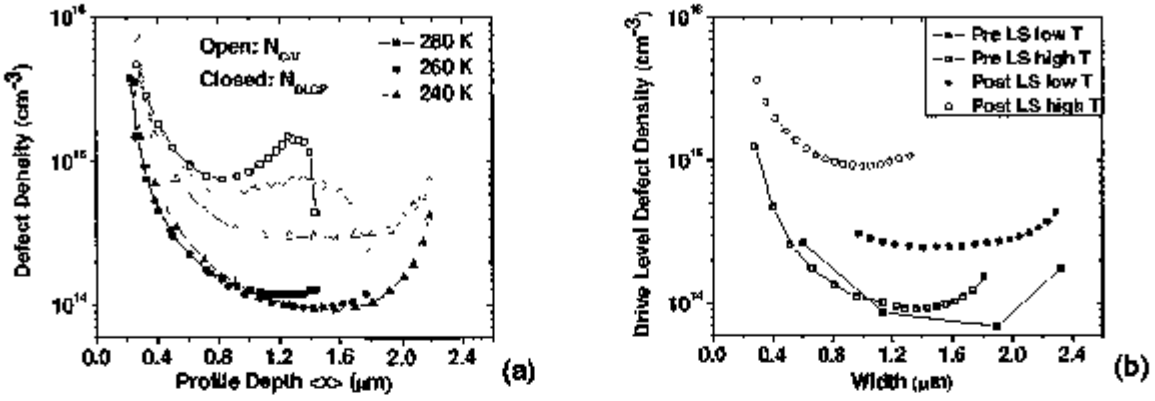

Figure 2 (a). Drive level capacitance and C-V profiles of 30% Ga, 28% Ag sample indicating the very low free carrier density. (b) After light soaking, the free carrier density increases and a level indicative of a deep defect becomes evident in the DLCP profiles at higher temperature.

profile is typical for all of the ACIGS samples, showing a free carrier density near 10^{14} cm^{-3} and little or no deep defect response from DLCP when the sample is in its annealed state. After the sample has been light soaked, the free carrier density increases to near $3x10^{14}$ cm^{-3} and a deep defect is very evident with a density of $7x10^{14}$ cm^{-3}. As indicated in Table I, all ACIGS samples had free carrier densities between $7x10^{13}$ cm^{-3} and $2x10^{14}$ cm^{-3}. When we compare the DLC profiles to standard C-V profiles as in Fig. 2(a), the C-V profiles reveal much higher values. This probably indicates a substantial number of electrically active defects near the CdS/ACIGS junction [8].

Transient photocapacitance spectroscopy can reveal information about the sub-band gap defect structure of a material as well as the amount of structural and compositional disorder that is present. One might expect that by adding another element to the CIGS lattice, we would find an increase in the Urbach energy, indicating that the structural disorder had increased. On the other hand, $AgInSe_2$ has a lower melting point than $CuInSe_2$, so one might expect a greater degree of structural relaxation and thus less disorder. As shown in figure 3 for the 16% Ag containing samples, it turns out that the latter is in fact correct. The Urbach energies of the ACIGS samples are much steeper than those of the CIGS counterparts, typically between our

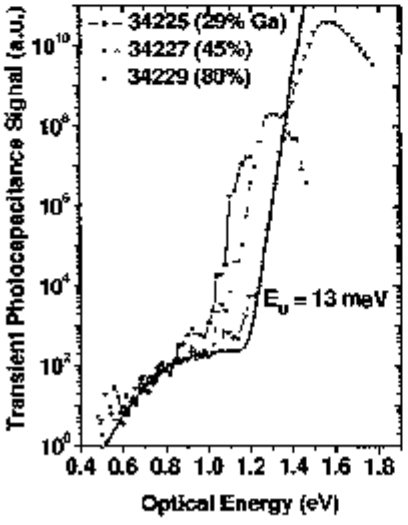

Figure 3: Transient photocapacitance spectra of 16% Ag ACIGS samples with varying amounts of Ga. The characteristic slope of the exponential band tail (Urbach edge) is between 10 meV and 20 meV in these samples, much steeper than in corresponding CIGS samples without Ag. This suggests that the Ag is somehow reducing the amount of structural disorder in the sample. The sub band gap defect signal (shoulder feature) can be fit with a defect centered near 0.8 eV in all of the spectra, similar to the defect signal found in CIGS.[9]

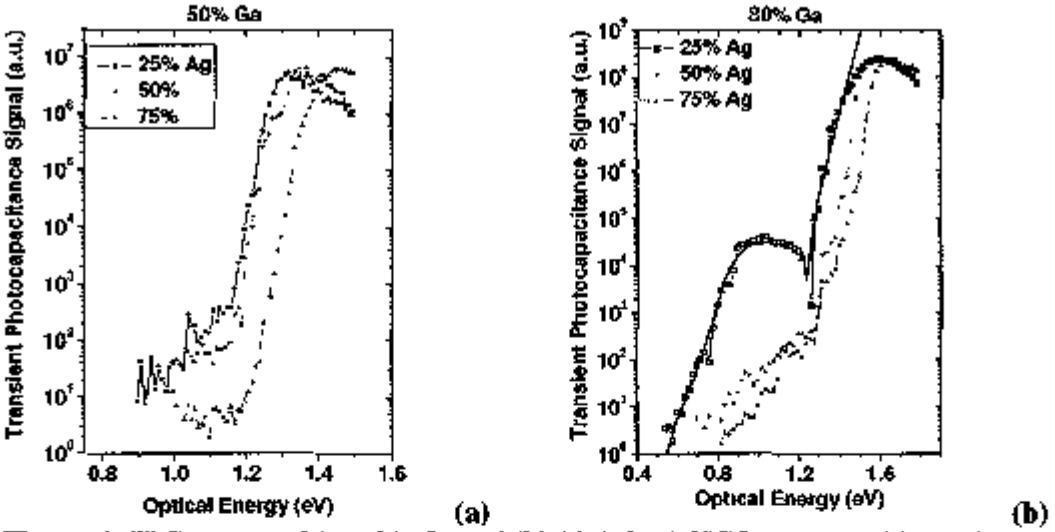

Figure 4: TPC spectra of (a) 50% Ga and (b) 80% Ga ACIGS samples with varying Ag content. The series show evidence of increasing band gap and decreasing defect signal with increasing Ag content. Note the spectrum of the 25% Ag sample in figure 4(b). The open symbols represent a TPC sign change, and the spectrum is well fit by an integral over a broad defect band. This may indicate that the material is actually bi-phase, as the transition occurs at the band gap of $AgInSe_2$ (1.24 eV).

resolution limit of 10 meV and 15 meV as opposed to 18-30 meV for CIGS.[9] The sub-band-gap defect signal is very similar to that seen in CIGS; namely, a gaussian distribution centered near 0.8 eV that appears to fit the shoulder feature in the TPC spectra for 16% Ag samples at all Ga concentrations.

Figure 4 shows the corresponding TPC spectra for the sample varying Ag content and with the higher Ga concentrations, 50% and 80%. Both sets of samples show higher open circuit voltages as the Ag fraction is increased from 25% to 75%. The TPC spectra show that the band gap increases with increasing Ag, which may explain the increase in V_{OC}.

The 80% Ga, 25% Ag sample exhibits a feature distinct from the rest of the ACIGS samples. Above the band gap to halfway down the band-tail, the TPC signal is positive but then, at 1.24 eV the TPC signal switches sign and becomes negative, as indicated by the open symbols. One interesting interpretation is that this sample is actually a mixed phase material containing small inclusions of $AgInSe_2$ (the transition at 1.24 eV coincides with the band gap of $AgInSe_2$). However, the volume fraction indicated from Fig. 4(b) for this phase would be very small, less than 0.01%.

DISCUSSION

As indicated by the IV data and the TPC spectra, alloying Ag into CIGS provides two mechanisms to potentially increase the V_{OC} of CIGS solar cell devices. First, the band gap of ACIGS devices appears to increase with the addition of Ag by up to 0.2 eV, depending on the Ag content. The Ag also appears to reduce the amount of structural disorder in the sample, as evidenced by the extremely low Urbach edges between 10 meV and 15 meV. This should allow the quasi-Fermi levels under illumination to move closer to the band edges before they are limited by the large density of states in the band-tails, thus leading to higher values of V_{OC}. However the inclusion of Ag also appears to decrease the carrier density to the point of being

detrimental to device performance. Although there is no deep defect apparent in the ACIGS samples when they are in a fully annealed state, light soaking reveals a defect with activation energies near 200 meV, very similar to the defect present in CIGS without Ag. This metastable defect also anneals at a similar temperature and time scale as the defect in CIGS, indicating that the atomic structure of the defect is most likely also similar. The TPC spectra of the 81% Ga, 27% Ag sample, which shows a unique transition from a majority carrier process to a minority carrier process, may indicate that this may actually be a bi-phase material. One possible explanation is the inclusion of $AgInSe_2$ crystallites in the CIGS, since the transition takes place at exactly the band gap of $AgInSe_2$. This does not imply that future ACIGS samples with similar compositions will also exhibit such a mixed phase character. However, this example does demonstrate the power of the TPC method to uncover subtle sample inhomogeneities.

CONCLUSIONS

We have successfully alloyed Ag into CIGS thin film photovoltaic solar cells over a broad range of compositions. Only one of the ten samples we examined exhibited evidence of a possible low level of phase separation within the film. Drive level capacitance profiling has revealed very low free carrier concentrations in the films, varying from $7x10^{13}$ cm^{-3} to $2x10^{14}$ cm^{-3}. Transient photocapacitance spectroscopy exhibited Urbach edges of 10 meV to 15 meV, much steeper than those of CIGS which normally lie between 18 and 30 meV. After samples were light soaked with AM 1.5 white light, the free carrier concentration increases and an activated defect appeared with a characteristic energy between 150 meV and 250 meV (depending on the sample), very similar to the behavior of CIGS without Ag. The open circuit voltage of the 50% and 80% Ga samples increased as the Ag content was increased from 25% to 75%. Thus, alloying CIGS with Ag may indeed provide a way to increase device performance, partially overcoming the well documented V_{OC}-deficit found in high Ga CIGS devices.

ACKNOWLEDGEMENTS

This work was supported under DOE contract # DE-FC36-08GO18019. PTE acknowledges support from the NSF IGERT program no. DGE-0549503.

REFERENCES

[1] W. N. Shafarman, R. Klenk, and B. E. McCandless, J. Appl. Phys. 79 (1996) 7324.
[2] J. L. Shay and J. H. Wernick, *Ternary Chalcopyrite Semiconductors: Growth, Electronic Properties, and Applications* (Pergamon Press, Oxford, 1975).
[3] M. Robbins, J. C. Phillips, and V. G. Lambrecht, Journal of Physics and Chemistry of Solids 34 (1973).
[4] J. E. Avon, K. Yoodee, and J. C. Woolley, J. Appl. Phys. 55 (1984).
[5] T. Nakada, K. Yamada, R. Arai, H. Ishizaki, and N. Yamada, Mater. Res. Soc. Symp. Proc. 865 (2005).
[6] J. T. Heath, J. D. Cohen, and W. N. Shafarman, J. Appl. Phys. 95 (2004) 1000.
[7] J. D. Cohen, J. T. Heath, and W. N. Shafarman, in: U. Rau and S. Siebentritt (Eds.), Wide Gap Chalcopyrites, Springer, Berlin, 2005, p. 69-90.
[8] P. T. Erslev, J. W. Lee, W. N. Shafarman, and J. D. Cohen, Thin Solid Films 517 (2009).
[9] J. T. Heath, J. D. Cohen, W. N. Shafarman, D. X. Liao, and A. A. Rockett, Appl. Phys. Lett. 80 (2002).